Gold-Nanoparticle-Based Colorimetric Discrimination of Cancer-Related Point Mutations with Picomolar Sensitivity

Paola Valentini,[†] Roberto Fiammengo,[†] Stefania Sabella,[†] Manuela Gariboldi,[‡,§] Gabriele Maiorano,[†] Roberto Cingolani,[⊥] and Pier Paolo Pompa[†,*]

[†]Center for Bio-Molecular Nanotechnologies@UniLe, Istituto Italiano di Tecnologia, Via Barsanti-73010 Arnesano (Lecce), Italy, [‡]Department of Experimental Oncology and Molecular Medicine, Fondazione IRCCS Istituto Nazionale dei Tumori, Milano, Italy, [§]Fondazione Istituto FIRC Oncologia Molecolare (IFOM), Milano, Italy, and [⊥]Istituto Italiano di Tecnologia, Via Morego, 30-16136 Genova, Italy

ABSTRACT

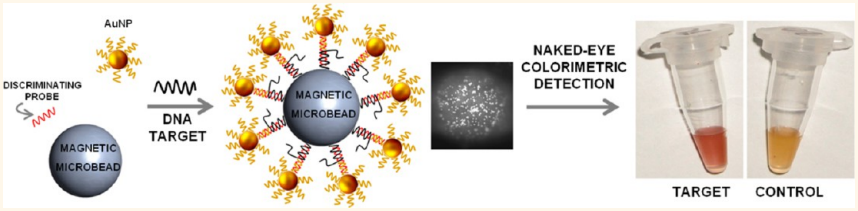

Point mutations in the Kirsten rat sarcoma viral oncogene homologue (KRAS) gene are being increasingly recognized as important diagnostic and prognostic markers in cancer. In this work, we describe a rapid and low-cost method for the naked-eye detection of cancer-related point mutations in KRAS based on gold nanoparticles. This simple colorimetric assay is sensitive (limit of detection in the low picomolar range), instrument-free, and employs nonstringent room temperature conditions due to a combination of DNA-conjugated gold nanoparticles, a probe design which exploits cooperative hybridization for increased binding affinity, and signal enhancement on the surface of magnetic beads. Additionally, the scheme is suitable for point-of-care applications, as it combines naked-eye detection, small sample volumes, and isothermal (PCR-free) amplification.

KEYWORDS: biosensors · colorimetric · genotyping · gold nanoparticles · stacking interactions

Point mutations in codons 12 and 13 of KRAS are very common in different types of cancers and have been widely shown to be associated with a poor prognosis. It has been estimated that 17−25% of all cancers harbor mutations in this gene;[1] in particular, these are present in 90% of all pancreas cancers, 33% of non-small cell lung cancer (NSCLC),[2] and ∼40% of metastatic colorectal cancers (mCRC).[3] Two mutations at codon 12 of the gene (35G>A and 35G>T) account together for 58% of all KRAS mutations found in cancer.[3] In mCRC, the presence of these KRAS mutations has also been associated with more aggressive metastatic behavior[4] and failure to respond to antibody therapies (cetuximab and panitumumab) targeting the epithelial growth factor receptor (EGFR).[1] Determination of KRAS mutation status is, thus, of crucial importance for therapeutic decisions in the treatment of metastatic colon cancer. In 2009, the American Society of Clinical Oncology (ASCO) stated a provisional clinical opinion, asserting that KRAS mutation testing should be mandatory for all patients with metastatic colon cancer before undergoing EGFR antibody therapy.[5] Currently, 12 KRAS mutation test kits, which conform to the requirements of the EU IVD Directive 98/79/EC, are available as diagnostic tools on the European market.[6] These tests can be distinguished in three categories, based on their underlying working principle, namely, real-time PCR, DNA hybridization, or sequencing.[6] However, the major limitation to large-scale utilization of these kits is their elevated cost per sample and the requirement for expensive instrumentation. Therefore, a device allowing cost-effective, rapid, and large-scale KRAS mutation screening may be very attractive for personalized therapy of cancer patients. Detection of point mutations in human genomic DNA with simple methodologies is quite

* Address correspondence to pierpaolo.pompa@iit.it.

Received for review April 10, 2013 and accepted May 22, 2013.

Published online May 22, 2013
10.1021/nn401757w

challenging.[7] Typically, it is necessary to include in the assay one or more key steps that may increase the number of variables affecting the final result and reduce assay simplicity; this may occur, for instance, when enzymatic reactions,[8−10] hairpin probes,[9] additional separation and cleaning steps or melting curve analyses[10,11] are employed.

In this work, we demonstrated colorimetric detection of the cancer-related point mutation 35G>A in KRAS due to the use of gold nanoparticles (AuNPs) combined with signal enhancement on the surface of paramagnetic microparticles. AuNPs are increasingly used as biosensing elements due to their interesting optical properties.[12−17] In particular, they have been used in several colorimetric detection schemes, generally exploiting their color change upon aggregation.[18−25] Here, a sensitive and rapid discrimination of the single mismatch under nonstringent salt conditions and at room temperature was obtained due to the combination of three factors: (i) the enhancement of the binding affinities due to cooperative hybridization of oligonucleotides;[26,27] (ii) the sharp melting transitions characterizing AuNP-conjugated DNA probes;[18,28] (iii) the relatively large nanoparticle size (40 nm), which renders the assay very sensitive, allowing for naked-eye detection. This simple, cost-effective, and instrument-free detection scheme is suitable for point-of-care (POC) devices. In view of the development of such platforms, we chose, for the target amplification step, the helicase-dependent isothermal amplification (HDA),[29] which permitted us to avoid the complexity of thermal cycles associated with traditional PCR, while maintaining an amplification efficiency comparable to the latter.

RESULTS

Isothermal Amplification of KRAS. A KRAS fragment of 101 base pairs was amplified from genomic DNA extracted from HT29 wild-type (wt) or LS180 mutant (mut) cell lines by means of HDA. This technique utilizes a DNA helicase and single-stranded DNA binding proteins (ssBPs) in order to open the double helix, thus avoiding the need for thermal denaturation of the template.[29] The amplification efficiency of the isothermal reaction was similar to that of a traditional PCR. No unspecific amplification was observed (Figure 1). The amplification was obtained at 65 ± 2 °C, suggesting that the reaction tolerates slight changes in temperature very well. This is a favorable aspect for potential applications of this assay in point-of-care devices, relying on simple instrumentation and not requiring complex thermal cycles.

Colorimetric Discrimination of Point Mutations in KRAS. Figure 2 describes the reaction scheme adopted in this study. The isothermally amplified KRAS fragment incorporates one biotin molecule (through the reverse primer), so that it can be captured by the streptavidin-modified paramagnetic microparticles. As the PCR

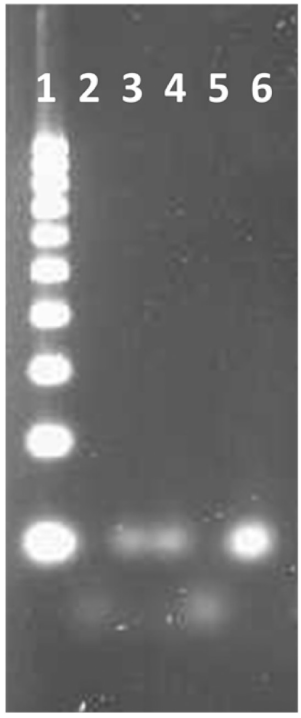

Figure 1. Isothermal amplification of KRAS target. Lane 1: 1Kb marker. Lanes 2 and 5: negative controls. Lanes 3 and 4: 101 bp amplified KRAS target. Lane 6: internal positive control of the kit.

product is double-stranded, the interfering complementary strand has to be displaced, which is obtained by incubation and washing in basic environment. Then, the discriminating probe (Table 1) can bind to the biotinylated single strand with its 5′ portion and can bind the AuNP-conjugated detection probe (poly(T)) with its 3′ poly(A) tail. During the hybridization, both the mixture containing the perfectly matched probe and target and the mixture containing single mismatched pairs appear red. The nonhybridized AuNP probes are then removed by magnetic separation. Already after the first washing step, the sample containing a single mismatch between the probe and the target starts losing its red color and exhibits a yellow background at the end of the third washing step. Notably, this naked-eye discrimination of a single point mutation can be achieved under nonstringent salt conditions, at room temperature and in about 90 min. Figure 3 shows the visual colorimetric detection of the 35G>A point mutation in the amplified KRAS target and the relative instrumental characterization. When KRAS amplified from the homozygous wt cell line HT29 is used, hybridization with the perfectly matched wt probe results in an intense red coloration of the magnetic beads, due to sandwich hybridization of AuNP−DNA probes. When the same target is tested with the probe specific for the 35G>A mutation, the color of the beads remains yellow, indicating that the AuNP probes, in the presence of a single mismatch, are not retained onto the beads' surface after magnetic washing (Figure 3A).

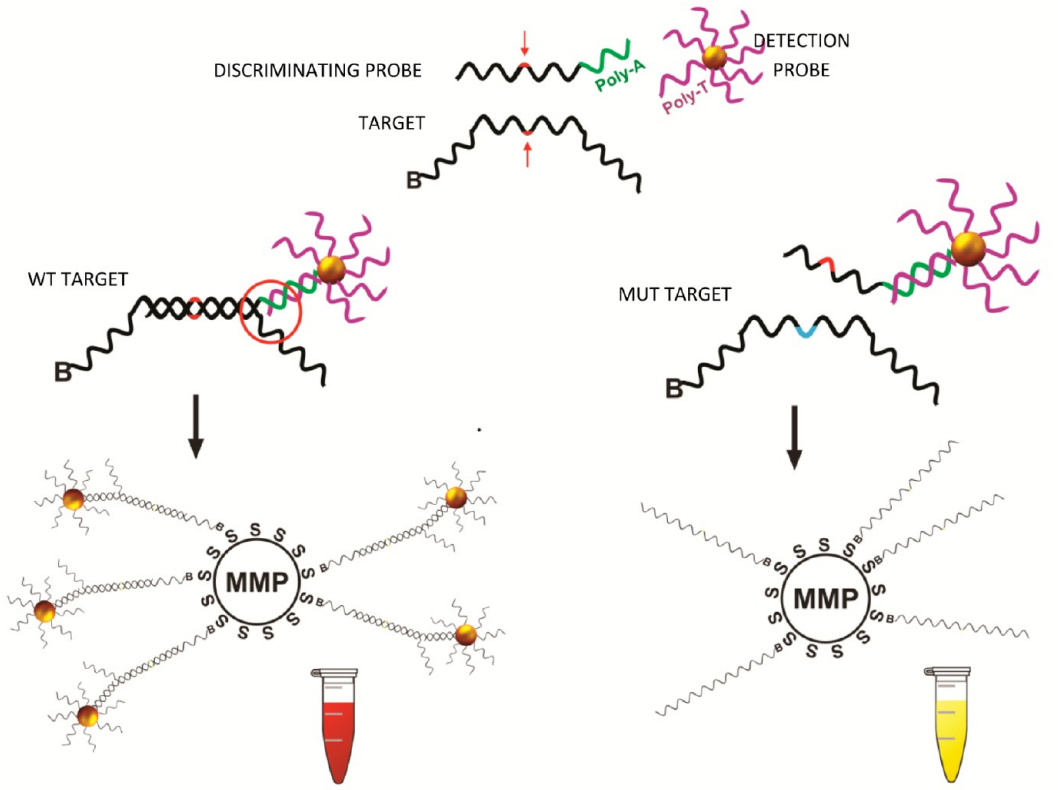

Figure 2. Reaction scheme of the KRAS genotyping assay. When discriminating probe and target are perfectly matched (left), the probe binds both the biotinylated target with its 5′ portion and the AuNP probe with its poly(A) 3′ portion, and cooperative binding stabilizes the hybrid (red circle). This complex, captured by the streptavidin-modified paramagnetic beads, gives a red color to the suspension due to the presence of the AuNPs. On the other side (right), a point mutation in the target (light blue) impairs the proper hybridization of the probe with the target, so that the AuNP probes are washed away during magnetic separation, resulting in a background yellow color (due to the magnetic beads). Abbreviations: MMP, paramagnetic microparticle; S, streptavidin; B, biotin.

TABLE 1. Sequence of Probes and Primers (Position of the Point Mutation Is Underlined)

name	sequence	function
probe wt	5′AGCTG**G**TGGCGTAGGpoly(A)$_{30}$3′	discriminating probe
probe 35G>A	5′AGCTG**A**TGGCGTAGGpoly(A)$_{30}$3′	discriminating probe
FW primer	5′AGGCCTGCTGAAAATGACTGAA3′	primer
REV primer	5′biotin-CCACAAAATGATTCTGAATTAGCTGTA3′	primer
AuNP probe	5′SH-(O-CH$_2$-CH$_2$)$_3$-T$_{(30)}$3′	detection probe

Interestingly, when KRAS is amplified from the cell line LS180, heterozygous for the 35G>A mutation, an intermediate orange color is observed upon hybridizing the target with either the wt or the 35G>A mut discriminating probes (Figure 3B). A heterozygous cell line can, thus, be distinguished from a homozygous wt or a mutant cell line, which will give a positive signal (red) only with the matched probe. UV−vis spectra of the matched and mismatched samples confirmed the naked-eye inspection, showing a considerable red shift of the absorbance of the beads upon target-induced binding of the AuNP probes. A calibration curve derived from the UV−vis spectra is shown in Supporting Information (Figure S1). The differential spectrum (matched minus mismatched sample) is consistent with the plasmon absorption of AuNPs (Figure 3C). ICP-AES analysis indicates that the gold/iron ratio in samples containing a wt copy of KRAS hybridized with a perfectly matched probe is considerably higher than in samples with a single mismatch (Figure 3D), confirming that the red color observed in the first case is actually due to the AuNPs. Finally, SEM (Figure 3E, F) and TEM images (Figure 3G) clearly show a large number of AuNPs decorating the surface of the paramagnetic beads in samples containing the perfectly matched target and probe pairs, unlike samples with a single mismatch. The assay was comparably efficient when using targets amplified by traditional PCR or helicase-dependent isothermal amplification (Supporting Information, Figure S2). Notably, the amount of isothermally amplified product necessary for the reaction was as low as 3 μL, without additional purification or processing steps. Working with small volumes of samples is important in view of point-of-care lab-on-chip applications. In order to assess the sensitivity of the method, the amplified target was first quantified by UV spectrophotometry, after purification by polyacrylamide gel electrophoresis, in order to eliminate the non-elongated primers, which could interfere with UV quantification. Then, 32 fmol of amplified target was incubated with the

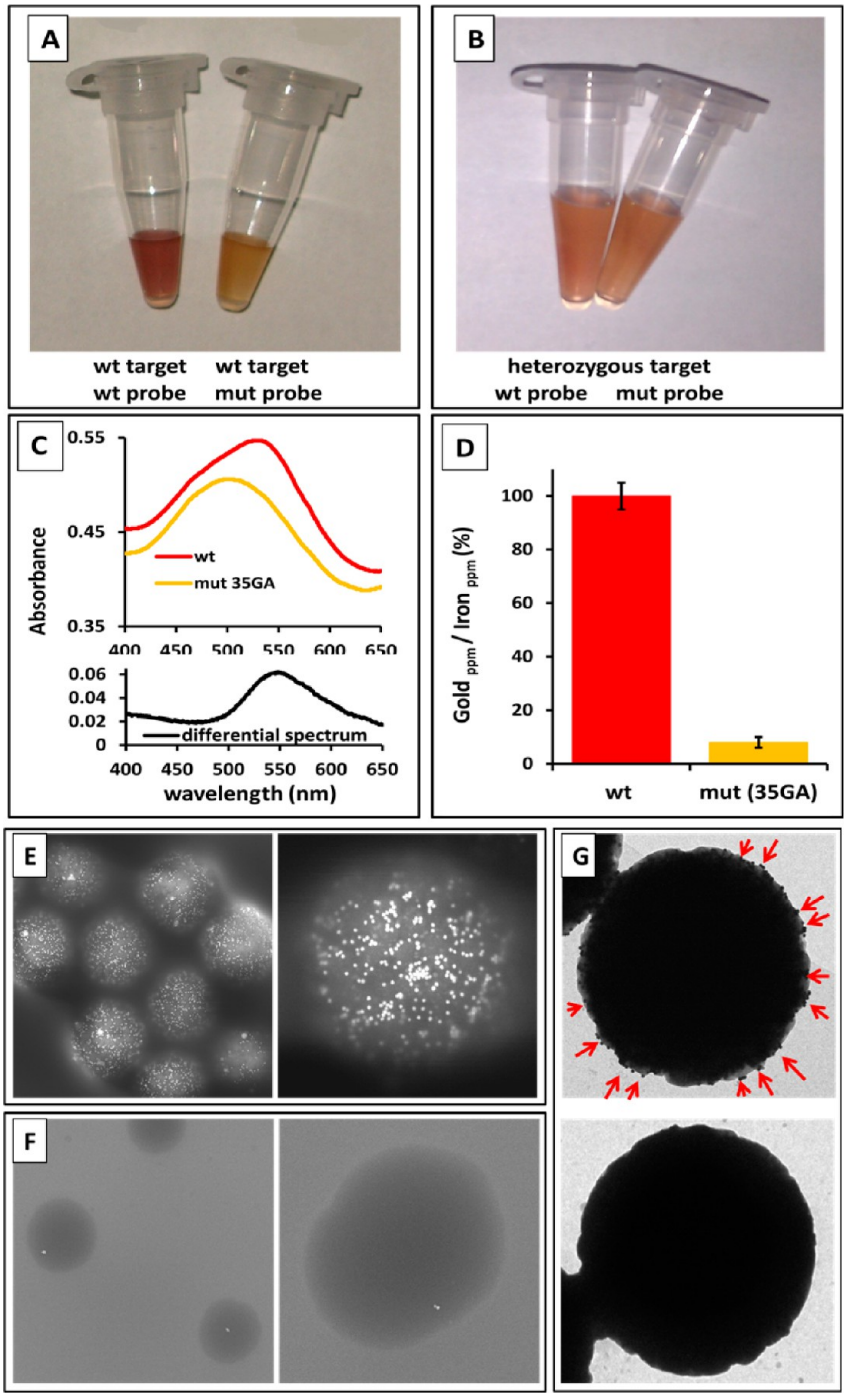

Figure 3. Discrimination of the cancer-related mutation 35G>A in KRAS. (A) Naked-eye discrimination of point mutation 35G>A. (B) Heterozygous cell line hybridizes partially with both wt and mutant probes, giving an intermediate color (orange). (C) UV–vis spectra of wt and mut samples, and differential spectrum (wt minus mut spectra). (D) ICP measurement of gold and iron in samples containing wt or point-mutated target. (E) SEM images of the magnetic beads after hybridization with target and AuNP probes. In samples containing wt target, the magnetic beads are decorated with several AuNPs (brilliant dots). (F) In samples containing point-mutated targets, only rare AuNPs bind the magnetic beads. (G) TEM images of samples containing wt target (top picture) and point-mutated target (bottom picture). Arrows highlight AuNP probes hybridized on matched target on the surface of magnetic beads.

streptavidin-modified beads at various concentrations, ranging from 1 nM to 10 pM. A clear red color (thus, a naked-eye discrimination of the point mutation) was observed in the presence of the perfect match, down to a target concentration as low as 20 pM (Supporting Information, Figure S3).

Effect of Cooperative Hybridization of Oligonucleotides and AuNP Probes. As shown in Figure 2, in our strategy, the AuNP-conjugated detection probe and the target bind to adjacent positions on the discriminating probe molecule. This design allows us to exploit the enhancement in binding affinities due to base pair stacking

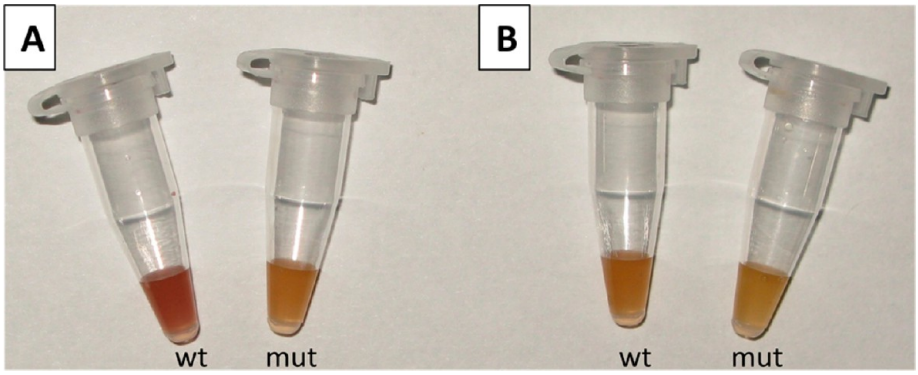

Figure 4. Effect of cooperative hybridization of oligonucleotides. (A) Discriminating probe and the detection probe are allowed to hybridize together, and a clear discrimination of the single point mutation is achieved in 70 min. (B) Discrimination probes is incubated alone for 1 h with the target, then after a washing step, the detection probe is added and incubated for an additional 1 h, so that parallel cooperative hybridization is not possible. Notwithstanding the longer incubation time, almost no discrimination of the point mutation is achieved in B, indicating that the binding affinity of the first probe alone, at room temperature and in the assay conditions, is not enough to detect the target, and that the enhancement of stability due to cooperative hybridization is necessary for detection.

interactions.[26,27] To assess whether cooperative hybridization of oligonucleotides was indeed affecting the stability of the final target–probe complex and the assay readout, parallel cooperative binding of the two probes was compared to sequential noncooperative binding of the same probes. When the discriminating probe and the detection probe were allowed to hybridize at the same time with the target (for a total hybridization time of 70 min), a clear colorimetric discrimination of a single mismatch was obtained (Figure 4). On the other side, if the two probes were hybridized sequentially, introducing a washing step between the first and the second hybridization, the colorimetric discrimination of the single mismatch was considerably less evident (although the total hybridization time was doubled). This suggests that this short 15 nucleotide (nt) discriminating probe, under the assay conditions, did not stably bind even a perfectly matched target and was largely rinsed away during the washing step. On the contrary, cooperative interactions between the two probes hybridizing at the same time with the target strongly stabilize the binding. Therefore, point mutation discrimination could be achieved at room temperature and under nonstringent salt conditions due to the combination of enhanced binding affinity promoted by cooperative hybridization of oligonucleotides and sharp melting transitions associated with AuNP probes.

DISCUSSION

KRAS mutations are routinely detected by allele-specific quantitative PCR or traditional PCR coupled to direct sequencing or pyrosequencing.[30] Many PCR-based assays for mutant allele discrimination have been described, as it seems convenient to combine the target amplification step with the discrimination of the mutation.[31–35] However, most of these methods require additional processing steps (restriction enzyme digestions, nested PCR, melting curve analysis), stringent hybridization conditions, and often specific instrumentation (HPLC, laser scanners, mass spectrometry, real-time PCR devices, fluorometers, capillary gel electrophoresis, luminometers, *etc.*) for the readout of the result, reducing simplicity and increasing costs, which is not desirable when thinking of a method for fast and large-scale population screening.

In our study, the target amplification is isothermal, thus considerably simpler when compared to traditional PCR or real-time PCR, as it can be performed without dedicated instrumentation, by simply keeping the temperature at ~65 °C for 2 h. Among the different isothermal amplification techniques reported in the literature, we chose HDA. HDA was particularly suitable for our system, as it does not require post-amplification processing steps, it can directly amplify a complex template such as human genomic DNA, and it has an optimal target length (around 100 nt) in a favorable range for a sandwich hybridization. Notably, this isothermal target amplification step is not involved in the mutation discrimination, which is performed in the colorimetric detection step. Moreover, the volume of amplified product required for the subsequent hybridization step is just 3 μL, which makes the assay potentially adaptable to a microfluidic platform for point-of-care applications. In the following detection step, discrimination by naked eye of a single mutation (35G>A) in the KRAS gene is achieved at room temperature, in less than 2 h, and under nonstringent conditions using magnetic microparticles and DNA-conjugated AuNPs, reaching a very low limit of detection (20 pM). The combination of different factors contributes to the high sensitivity of this method: (1) short discriminating probes enable the discrimination of a point mutation at room temperature; (2) cooperative hybridization of two probes confers enhanced binding stability to the perfectly matched probe–target duplex at the assay conditions; (3) AuNP probes (40 nm) enhance the visual

color detection; (4) signal enhancement on the surface of paramagnetic microparticles increases the naked-eye discrimination of the different colors, even when starting from diluted samples.

Several colorimetric methods exploited the distance-dependent color change caused by AuNP aggregation upon recognition of a target nucleic acid. Mirkin's group first demonstrated a colorimetric detection scheme based on AuNP aggregation to achieve single mismatch discrimination. The concentration of the synthetic target tested in this proof-of-concept experiment was of 60 nM.[18] Thereafter, many groups exploited the same principle to achieve naked-eye discrimination of single or multiple point mutations. The simpler schemes based on nanoparticle aggregation only reached sensitivities in the nanomolar range.[10,36−39] Other reports introduced an extra step of melting curve analysis to improve sensitivity in the mismatch discrimination.[40] Our method for single mismatch discrimination reaches high sensitivity, approaching that of studies where multiple mismatches or a fully noncomplementary sequence was discriminated from a wt target.[41,42]

Diverse works reported the enzymatic colorimetric discrimination of point mutations or single nucleotide polymorphisms. However, simpler methods are often proof-of-principle studies with low sensitivity. On the other hand, many studies applied to real clinical samples required sample processing steps employing dedicated instrumentation or strict control of the hybridization stringency conditions. Ausch *et al.*, for instance, detected KRAS mutations in cancer tissue samples using mutant-enriched PCR, array hybridization, and an enzymatic system for colorimetric readout.[43] In this case, standard hybridization required stringency wash and strict temperature control, which are not necessary in our settings due to the use of AuNP probes and to a probe design which exploits short oligonucleotide probes and enhanced stability through cooperative hybridization of adjacent probes. Other studies avoided the stringency hybridization conditions necessary for the discrimination of a point mutation by coupling a ligation step to AuNP aggregation.[21] When ligase was used in a PCR-like fashion, with the ligation chain reaction (LCR), it also allowed reaching high sensitivity.[44] Unfortunately, LCR requires thermal cycles, simplified but conceptually similar to a traditional PCR, which we chose to avoid in view of low-cost point-of-care applications.

Our system uses paramagnetic microbeads to enhance the colorimetric signal of the AuNPs. Other authors have exploited, previously, a combination of microbeads and AuNPs for the colorimetric detection of the presence of a synthetic DNA target[45] or the discrimination of a two-base mismatch.[46] However, the discrimination of a single-base mismatch was not attempted in these studies.

In most of the reports employing AuNP-conjugated DNA probes, DNA sequences specific for the target of interest are conjugated to the AuNPs. Therefore, for each new target, a specific functionalized nanoparticle has to be prepared. One of the advantages of our system is the use of universal poly-T AuNP probes, which make our assay quickly adaptable to any target by simply designing a new discriminating sandwich probe. This is much cheaper than preparing new functionalized AuNPs for each target and simplifies multiplexing applications. A previous work by Wilson's group obtained a colorimetric detection based on universal AuNP probes by conjugating an intercalating agent to AuNPs and could identify 25 pmol of target DNA.[47] In comparison, our assay is significantly more sensitive, as it can detect down to 32 fmol of DNA.

CONCLUSIONS

Our colorimetric assay is up to 4 orders of magnitude more sensitive than other as-simple AuNP-based colorimetric assays for single mismatch discrimination.[10,36−39] The complete assay, from isothermal target amplification to colorimetric readout in the presence or absence of the single-base mismatch, can be performed without costly instrumentation, requiring only a very simple heating device. Moreover, very small sample volumes are needed, so that the assay is easily adaptable to lab-on-chip platforms for point-of-care diagnostics, currently under development at our laboratory. Finally, the assay employs universal detection probes and can thus be easily adapted to multiplexed genotyping of KRAS or to other relevant diagnostic targets. For instance, a small panel of mutations can be screened simultaneously by hybridizing the amplified gene with different discriminating probes, each specific for a given mutation. Upon hybridization with the universal AuNP probe, a red coloration of the sample would indicate the presence of a specific mutation, which can quickly give an indication of the disease progression and help therapeutic decisions.

The sensitivity of the assay could be further improved by introducing a metal enhancement step,[48] which might allow the direct colorimetric genotyping of unamplified genomic DNA samples, as also demonstrated by other authors on array hybridization.[49,50]

MATERIALS AND METHODS

Synthesis of 40 nm Gold Nanoparticles. The 40 nm citrate-capped AuNPs were prepared as previously reported.[51] The obtained AuNPs were characterized by UV−vis spectrophotometry, DLS, TEM, and SEM (Supporting Information, Figure S4).

Conjugation of AuNPs with DNA Probes. AuNP-conjugated DNA probes were prepared according to published protocols.[52−54] Briefly, thiolated probe oligonucleotides ($T_{(30)}$-(O-CH_2-CH_2)$_3$-SH), purchased from IDT DNA, were digested with 10 mM tris(2-carboxyethyl)phosphine (TCEP) for 3 h at room temperature. The digested oligonucleotides were then incubated with 40 nm AuNPs in a 2000:1 molar ratio overnight, at room temperature, under mild shaking. The AuNP−DNA mixture was then brought to 0.3 M NaCl in 10 mM phosphate buffer, pH 7.4, 0.01% SDS, with stepwise increment of salt over the course of 8 h. After an additional overnight incubation at room temperature, the DNA-conjugated AuNPs were centrifuged and washed with 0.3 M NaCl in 10 mM phosphate buffer plus 0.01% SDS, in order to remove the excess unbound DNA. These probes were stored at 4 °C until their use. To determine the density of DNA probes on the nanoparticle surface, 10 μL of these DNA-conjugated AuNPs was digested overnight with 1 mM DTT in 90 mM phosphate buffer, pH 8, at 40 °C. The mixture was centrifuged at 13 400 rpm for 15 min in a benchtop centrifuge, and the amount of oligonucleotides in the supernatant was estimated using the Quant-iT OliGreen ssDNA kit (Invitrogen). The concentration of AuNPs was measured by UV−vis spectroscopy and inductively coupled plasma atomic emission spectroscopy (ICP-AES). On average, 686 $\pm$ 64 copies of probe oligonucleotide were found to be linked to each nanoparticle.

Cell Lines and Control of KRAS Status. The cell lines used were obtained from American Type Culture Collection (Manassas, VA). HT29 cells were maintained at 37 °C with 5% CO_2 and cultured in McCoy's 5A (Invitrogen) supplemented with 10% fetal bovine serum. LS180 cell lines were cultured in Eagle's minimum essential medium (Gibco) supplemented with 10% fetal bovine serum. Cells were tested and authenticated using the StemElite ID system (Promega). Mutational analysis of KRAS was done as previously described[55] using primers amplifying codon 12 of the gene.

Extraction of Genomic DNA from Cell Cultures. Genomic DNA was extracted from cultured cell lines HT29 (wt) and LS180 (heterozygous for mutation 35G>A) using DNeasy Blood & Tissue Kit (Qiagen). The concentration and purity of extracted DNA was measured using a UV spectrophotometer.

PCR and Helicase-Dependent Amplification. A 101 bp fragment including codons 12 and 13 in KRAS was amplified from genomic DNA using either a traditional PCR or a two-step isothermal amplification with the IsoAmp II Universal tHDA kit (Biohelix). Briefly, for PCR, reaction mixtures contained 100 ng of genomic DNA, 75 nM FW primer, 75 nM biotinylated REV primer, 2.5 mM $MgCl_2$, 1× PCR reaction buffer, and 0.5 μL of HotStart Taq (EuroClone). Thermal cycles were as follow: 15 min at 95 °C, followed by 30 cycles of 94 °C (1 min), 55 °C (1 min), 72 °C (1 min), and a final extension step of 10 min at 72 °C.

For HDA, 200 ng of template genomic DNA was denaturated for 5 min at 95 °C in the annealing buffer of the kit plus 75 nM FW primer and 75 nM biotinylated REV primer. The mixture was then placed on ice, and a reaction mix containing 3.5 μL of IsoAmp enzyme mix, 3.5 μL of IsoAmp dNTP solution, 40 mM NaCl, and 4 mM $MgSO_4$ in annealing buffer was added. This mixture was then incubated at 65 °C for 2 h. A 5 μL aliquot of the reaction was electrophoresed on a 2% agarose gel in 0.5% TBE to verify the presence of the desired amplicon and the absence of unspecific amplification.

Hybridization and Colorimetric Detection of Single Mismatch. Five microliters of Dynabeads M-280 streptavidin (Invitrogen) paramagnetic beads were washed twice with hybridization buffer (HB) (1× PBS pH 7.4 plus 5% w/v PEG 600), resuspended in an equal volume of HB, and incubated with a varying amount of biotinylated PCR or HDA product for 20 min at room temperature. The beads were then incubated with 0.15 M NaOH for 5 min to denaturate the double-stranded amplification product and magnetically separate the interfering nonbiotinylated strand. The beads were subsequently washed with 100 μL of 0.15 M NaOH and then with 100 μL of HB, then resuspended in 20 μL of HB. Then, 100 pmol of probe, recognizing the wt or point-mutated target, was added to the beads and incubated for 10 min at room temperature, then 100 fmol of DNA-conjugated AuNPs was added and incubated for 1 h at room temperature. The mixture was then washed three times with HB and the color readout ascertained visually. The UV−vis spectrum was also measured.

In experiments aimed at assessing the contribution of cooperative hybridization, the discriminating probe and the detection probe were either allowed to hybridize at the same time with the target or hybridized sequentially. In this latter case, the discriminating probe was added alone for 1 h, after which it was removed by magnetic separation. Then, after a washing step, the AuNP-conjugated detection probe was added and it was incubated with the beads for 1 h more. The sequences of all probes and primers used in this study are reported in Table 1.

ICP-AES Analysis. After the hybridization, 10 μL of each sample, containing wt or mutant target, was digested overnight with 500 μL of aqua regia (1 part nitric acid and 3 parts of hydrochloric acid). The next day, the mixture was diluted 100 times and ICP-AES analysis was performed using two different standard curves, one for gold and one for iron. The gold content in the two samples, resulting from the analysis, was normalized for the iron amount in each of them in order to avoid mistakes that might arise by any possible dis-homogeneity during sampling from the bead suspension.

Conflict of Interest: The authors declare no competing financial interest.

Acknowledgment. This work was partially supported by the Italian Flagship Project NanoMax and by a grant from Associazione Italiana Ricerca Cancro (AIRC) (IG 10529).

Supporting Information Available: Additional graphical data and images as described in the text. This material is available free of charge *via* the Internet at http://pubs.acs.org.

REFERENCES AND NOTES

1. Arrington, A. K.; Heinrich, E. L.; Lee, W.; Duldulao, M.; Patel, S.; Sanchez, J.; Garcia-Aguilar, J.; Kim, J. Prognostic and Predictive Roles of KRAS Mutation in Colorectal Cancer. *Int. J. Mol. Sci.* **2012**, *13*, 12153–12168.
2. Adjei, A. A. Blocking Oncogenic Ras Signaling for Cancer Therapy. *J. Natl. Cancer Inst.* **2001**, *93*, 1062–1074.
3. Neumann, J.; Zeindl-Eberhart, E.; Kirchner, T.; Jung, A. Frequency and Type of KRAS Mutations in Routine Diagnostic Analysis of Metastatic Colorectal Cancer. *Pathol. Res. Pract.* **2009**, *205*, 858–862.
4. Nash, G. M.; Gimbel, M.; Shia, J.; Nathanson, D. R.; Ndubuisi, M. I.; Zeng, Z. S.; Kemeny, N.; Paty, P. B. KRAS Mutation Correlates with Accelerated Metastatic Progression in Patients with Colorectal Liver Metastases. *Ann. Surg. Oncol.* **2010**, *17*, 572–578.
5. Allegra, C. J.; Jessup, J. M.; Somerfield, M. R.; Hamilton, S. R.; Hammond, E. H.; Hayes, D. F.; McAllister, P. K.; Morton, R. F.; Schilsky, R. L. American Society of Clinical Oncology Provisional Clinical Opinion: Testing for KRAS Gene Mutations in Patients with Metastatic Colorectal Carcinoma To Predict Response to Anti-epidermal Growth Factor Receptor Monoclonal Antibody Therapy. *J. Clin. Oncol.* **2009**, *27*, 2091–2096.
6. Domagala, P.; Hybiak, J.; Sulzyc-Bielicka, V.; Cybulski, C.; Rys, J.; Domagala, W. KRAS Mutation Testing in Colorectal Cancer as an Example of the Pathologist's Role in Personalized Targeted Therapy: A Practical Approach. *Pol. J. Pathol.* **2012**, *63*, 145–164.
7. Bichenkova, E. V.; Lang, Z.; Yu, X.; Rogert, C.; Douglas, K. T. DNA-Mounted Self-Assembly: New Approaches for Genomic Analysis and SNP Detection. *Biochim. Biophys. Acta* **2011**, *1809*, 1–23.
8. Hardenbol, P.; Yu, F.; Belmont, J.; Mackenzie, J.; Bruckner, C.; Brundage, T.; Boudreau, A.; Chow, S.; Eberle, J.; Erbilgin, A.; *et al.* Highly Multiplexed Molecular Inversion Probe Genotyping: Over 10,000 Targeted SNPs Genotyped in a Single Tube Assay. *Genome Res.* **2005**, *15*, 269–275.
9. Olivier, M.; Chuang, L. M.; Chang, M. S.; Chen, Y. T.; Pei, D.; Ranade, K.; de Witte, A.; Allen, J.; Tran, N.; Curb, D.; *et al.* High-Throughput Genotyping of Single Nucleotide Polymorphisms Using New Biplex Invader Technology. *Nucleic Acids Res.* **2002**, *30*, e53.

10. Chen, Y. T.; Hsu, C. L.; Hou, S. Y. Detection of Single-Nucleotide Polymorphisms Using Gold Nanoparticles and Single-Strand-Specific Nucleases. *Anal. Biochem.* **2008**, *2*, 299–305.
11. Mohammed, M. I.; Sills, G. J.; Brodie, M. J.; Ellis, E. M.; Girkin, J. M. A Complete Miniaturised Genotyping System for the Detection of Single Nucleotide Polymorphisms in Human DNA Samples. *Sens. Actuators, B* **2009**, *139*, 83–90.
12. Kreibig, U.; Genzel, L. Optical Absorption of Small Metallic Particles. *Surf. Sci.* **1985**, *156*, 678–700.
13. Grabar, K. C.; Smith, P. C.; Musick, M. D.; Davis, J. A.; Walter, D. G.; Jackson, M. A.; Guthrie, A. P.; Natan, M. J. Kinetic Control of Interparticle Spacing in Au Colloid-Based Surfaces: Rational Nanometer-Scale Architecture. *J. Am. Chem. Soc.* **1996**, *118*, 1148–1153.
14. Giljohann, D. A.; Seferos, D. S.; Daniel, W. L.; Massich, M. D.; Patel, P. C.; Mirkin, C. A. Gold Nanoparticles for Biology and Medicine. *Angew. Chem., Int. Ed.* **2010**, *49*, 3280–3294.
15. Dreaden, E. C.; Alkilany, A. M.; Huang, X.; Murphy, C. J.; El-Sayed, M. A. The Golden Age: Gold Nanoparticles for Biomedicine. *Chem. Soc. Rev.* **2012**, *41*, 2740–2779.
16. Orendorff, C. J.; Sau, T. K.; Murphy, C. J. Shape-Dependent Plasmon-Resonant Gold Nanoparticles. *Small* **2006**, *2*, 636–639.
17. Carregal-Romero, S.; Montenegro, J. M.; Parak, W. J.; Rivera Gil, P. Subcellular Carrier-Based Optical Ion-Selective Nanosensors. *Front. Neuropharmacol.* **2012**, *3*, 1–7.
18. Storhoff, J. J.; Elghanian, R.; Mucic, R. C.; Mirkin, C. A.; Letsinger, R. L. One-Pot Colorimetric Differentiation of Polynucleotides with Single Base Imperfections Using Gold Nanoparticle Probes. *J. Am. Chem. Soc.* **1998**, *120*, 1959–1964.
19. Reynolds, R. A.; Mirkin, C. A.; Letsinger, R. L. Homogeneous, Nanoparticle-Based Quantitative Colorimetric Detection of Oligonucleotides. *J. Am. Chem. Soc.* **2000**, *122*, 3795–3796.
20. Storhoff, J. J.; Lucas, A. D.; Garimella, V.; Bao, Y. P.; Muller, U. R. Homogeneous Detection of Unamplified Genomic DNA Sequences Based on Colorimetric Scatter of Gold Nanoparticle Probes. *Nat. Biotechnol.* **2004**, *22*, 883–887.
21. Li, J.; Chu, X.; Liu, Y.; Jiang, J. H.; He, Z.; Zhang, Z.; Shen, G.; Yu, R. Q. A Colorimetric Method for Point Mutation Detection Using High-Fidelity DNA Ligase. *Nucleic Acids Res.* **2005**, *33*, e168.
22. Oh, J. H.; Lee, J. S. Designed Hybridization Properties of DNA–Gold Nanoparticle Conjugates for the Ultraselective Detection of a Single-Base Mutation in the Breast Cancer Gene BRCA1. *Anal. Chem.* **2011**, *83*, 7364–7370.
23. de la Rica, R.; Stevens, M. M. Plasmonic ELISA for the Ultrasensitive Detection of Disease Biomarkers with the Naked Eye. *Nat. Nanotechnol.* **2012**, *7*, 821–824.
24. Lee, H.; Joo, S. W.; Lee, S. Y.; Lee, C. H.; Yoon, K. A.; Lee, K. Colorimetric Genotyping of Single Nucleotide Polymorphism Based on Selective Aggregation of Unmodified Gold Nanoparticles. *Biosens. Bioelectron.* **2010**, *26*, 730–735.
25. Qi, Y.; Li, B. A Sensitive, Label-Free, Aptamer-Based Biosensor Using a Gold Nanoparticle-Initiated Chemiluminescence System. *Chemistry* **2011**, *17*, 1642–1648.
26. Zhang, D. Y. Cooperative Hybridization of Oligonucleotides. *J. Am. Chem. Soc.* **2011**, *133*, 1077–1086.
27. Lane, M. J.; Paner, T.; Kashin, I.; Faldasz, B. D.; Li, B.; Gallo, F. J.; Benight, A. S. The Thermodynamic Advantage of DNA Oligonucleotide `Stacking Hybridization' Reactions: Energetics of a DNA Nick. *Nucleic Acids Res.* **1997**, *25*, 611–617.
28. Jin, R.; Wu, G.; Li, Z.; Mirkin, C. A.; Schatz, G. C. What Controls the Melting Properties of DNA-Linked Gold Nanoparticle Assemblies? *J. Am. Chem. Soc.* **2003**, *125*, 1643–1654.
29. Vincent, M.; Xu, Y.; Kong, H. Helicase-Dependent Isothermal DNA Amplification. *EMBO Rep.* **2004**, *5*, 795–800.
30. Dufort, S.; Richard, M. J.; de Fraipont, F. Pyrosequencing Method To Detect KRAS Mutation in Formalin-Fixed and Paraffin-Embedded Tumor Tissues. *Anal. Biochem.* **2009**, *391*, 166–168.
31. Levi, S.; Urbano-Ispizua, A.; Gill, R.; Thomas, D. M.; Gilbertson, J.; Foster, C.; Marshall, C. J. Multiple K-Ras Codon 12 Mutations in Cholangiocarcinomas Demonstrated with a Sensitive Polymerase Chain Reaction Technique. *Cancer Res.* **1991**, *51*, 3497–3502.
32. Clayton, S. J.; Scott, F. M.; Walker, J.; Callaghan, K.; Haque, K.; Liloglou, T.; Xinarianos, G.; Shawcross, S.; Ceuppens, P.; Field, J. K.; *et al.* K-Ras Point Mutation Detection in Lung Cancer: Comparison of Two Approaches to Somatic Mutation Detection Using Arms Allele-Specific Amplification. *Clin. Chem.* **2000**, *46*, 1929–1938.
33. Behn, M.; Thiede, C.; Neubauer, A.; Pankow, W.; Schuermann, M. Facilitated Detection of Oncogene Mutations from Exfoliated Tissue Material by a PNA-Mediated `Enriched PCR' Protocol. *J. Pathol.* **2000**, *190*, 69–75.
34. Luo, J. D.; Chan, E. C.; Shih, C. L.; Chen, T. L.; Liang, Y.; Hwang, T. L.; Chiou, C. C. Detection of Rare Mutant K-Ras DNA in a Single-Tube Reaction Using Peptide Nucleic Acid as Both PCR Clamp and Sensor Probe. *Nucleic Acids Res.* **2006**, *34*, e12.
35. Kriegshauser, G.; Fabjani, G.; Ziegler, B.; Zochbauer-Muller, S.; End, A.; Zeillinger, R. Biochip-Based Detection of KRAS Mutation in Non-Small Cell Lung Cancer. *Int. J. Mol. Sci.* **2011**, *12*, 8530–8538.
36. Taton, T. A.; Lu, G.; Mirkin, C. A. Two-Color Labeling of Oligonucleotide Arrays *via* Size-Selective Scattering of Nanoparticle Probes. *J. Am. Chem. Soc.* **2001**, *123*, 5164–5165.
37. Li, H.; Rothberg, L. Colorimetric Detection of DNA Sequences Based on Electrostatic Interactions with Unmodified Gold Nanoparticles. *Proc. Natl. Acad. Sci. U.S.A.* **2004**, *101*, 14036–14039.
38. Murphy, D.; O'Brien, P.; Redmond, G. Sub-Picomole Colorimetric Single Nucleotide Polymorphism Discrimination Using Oligonucleotide–Nanoparticle Conjugates. *Analyst* **2004**, *129*, 970–974.
39. Charrier, A.; Candoni, N.; Liachenko, N.; Thibaudau, F. 2D Aggregation and Selective Desorption of Nanoparticle Probes: A New Method To Probe DNA Mismatches and Damages. *Biosens. Bioelectron.* **2007**, *22*, 1881–1886.
40. Li, J.; Jiang, J. H.; Xu, X. M.; Chu, X.; Jiang, C.; Shen, G.; Yu, R. Q. Simultaneous Identification of Point Mutations *via* DNA Ligase-Mediated Gold Nanoparticle Assembly. *Analyst* **2008**, *133*, 939–945.
41. Xia, F.; Zuo, X.; Yang, R.; Xiao, Y.; Kang, D.; Vallee-Belisle, A.; Gong, X.; Yuen, J. D.; Hsu, B. B.; Heeger, A. J.; *et al.* Colorimetric Detection of DNA, Small Molecules, Proteins, and Ions Using Unmodified Gold Nanoparticles and Conjugated Polyelectrolytes. *Proc. Natl. Acad. Sci. U.S.A.* **2010**, *107*, 10837–10841.
42. Cordray, M. S.; Amdahl, M.; Richards-Kortum, R. R. Gold Nanoparticle Aggregation for Quantification of Oligonucleotides: Optimization and Increased Dynamic Range. *Anal. Biochem.* **2012**, *431*, 99–105.
43. Ausch, C.; Buxhofer-Ausch, V.; Oberkanins, C.; Holzer, B.; Minai-Pour, M.; Jahn, S.; Dandachi, N.; Zeillinger, R.; Kriegshauser, G. Sensitive Detection of KRAS Mutations in Archived Formalin-Fixed Paraffin-Embedded Tissue Using Mutant-Enriched PCR and Reverse-Hybridization. *J. Mol. Diagn.* **2009**, *11*, 508–513.
44. Shen, W.; Deng, H.; Gao, Z. Gold Nanoparticle-Enabled Real-Time Ligation Chain Reaction for Ultrasensitive Detection of DNA. *J. Am. Chem. Soc.* **2012**, *134*, 14678–14681.
45. Reynolds, R. A.; Mirkin, C. A.; Letsinger, R. L. A Gold Nanoparticle/Latex Microsphere-Based Colorimetric Oligonucleotide Detection Method. *Pure Appl. Chem.* **2000**, *72*, 229–235.
46. Chen, Y.; Aveyard, J.; Wilson, R. Gold and Silver Nanoparticles Functionalized with Known Numbers of Oligonucleotides Per Particle for DNA Detection. *Chem. Commun.* **2004**, 2804–2805.
47. Mehrabi, M.; Wilson, R. Intercalating Gold Nanoparticles as Universal Labels for DNA Detection. *Small* **2007**, *3*, 1491–1495.
48. Taton, T. A.; Mirkin, C. A.; Letsinger, R. L. Scanometric DNA Array Detection with Nanoparticle Probes. *Science* **2000**, *289*, 1757–1760.

49. Storhoff, J. J.; Marla, S. S.; Bao, P.; Hagenow, S.; Mehta, H.; Lucas, A.; Garimella, V.; Patno, T.; Buckingham, W.; Cork, W.; *et al.* Gold Nanoparticle-Based Detection of Genomic DNA Targets on Microarrays Using a Novel Optical Detection System. *Biosens. Bioelectron.* **2004**, *19*, 875–883.
50. Bao, Y. P.; Huber, M.; Wei, T. F.; Marla, S. S.; Storhoff, J. J.; Muller, U. R. SNP Identification in Unamplified Human Genomic DNA with Gold Nanoparticle Probes. *Nucleic Acids Res.* **2005**, *33*, e15.
51. Pompa, P. P.; Vecchio, G.; Galeone, A.; Brunetti, V.; Maiorano, G.; Sabella, S.; Cingolani, R. Physical Assessment of Toxicology at Nanoscale: Nano Dose-Metrics and Toxicity Factor. *Nanoscale* **2011**, *3*, 2889–2897.
52. Mirkin, C. A.; Letsinger, R. L.; Mucic, R. C.; Storhoff, J. J. A DNA-Based Method for Rationally Assembling Nanoparticles into Macroscopic Materials. *Nature* **1996**, *382*, 607–609.
53. Hurst, S. J.; Lytton-Jean, A. K.; Mirkin, C. A. Maximizing DNA Loading on a Range of Gold Nanoparticle Sizes. *Anal. Chem.* **2006**, *78*, 8313–8318.
54. Alhasan, A. H.; Kim, D. Y.; Daniel, W. L.; Watson, E.; Meeks, J. J.; Thaxton, C. S.; Mirkin, C. A. Scanometric MicroRNA Array Profiling of Prostate Cancer Markers Using Spherical Nucleic Acid−Gold Nanoparticle Conjugates. *Anal. Chem.* **2012**, *84*, 4153–4160.
55. Reid, J. F.; Gariboldi, M.; Sokolova, V.; Capobianco, P.; Lampis, A.; Perrone, F.; Signoroni, S.; Costa, A.; Leo, E.; Pilotti, S.; *et al.* Integrative Approach for Prioritizing Cancer Genes in Sporadic Colon Cancer. *Genes, Chromosomes Cancer* **2009**, *48*, 953–962.